

# Fluorescent gold nanoclusters as pH sensors for the pH 5 to 9 range and for imaging of blood cell pH values

Reham Ali<sup>1</sup> · Sayed M. Saleh<sup>2</sup> · Sanaa M. Aly<sup>3</sup>

Received: 12 March 2017 / Accepted: 29 May 2017 / Published online: 6 June 2017  
© Springer-Verlag Wien 2017

**Abstract** The authors describe the use of gold nanoclusters (AuNCs) with a diameter of ~2 nm for fluorescent sensing of pH values in the range from 5 to 9. The AuNCs were synthesized in the presence of bovine serum albumin (BSA) which acts as both a reducing agent and capping agent. The resulting AuNCs were characterized in terms of size and surface chemistry using TEM and FTIR. The BSA-capped AuNCs display red luminescence, with excitation/emission peaks at 470/640 nm, which is strongly modulated by the pH indicator bromothymol blue (BTB). The effect depends mainly on an inner filter effect due to spectral overlap between the absorption BTB and the emission of the AuNCs. The pH nanosensor responds to pH values in the range from 5 to 9 which is the so-called physiological pH range. The method was applied to detect changes in the pH values that occur after the death of red blood cells. Such pH changes are considered as a potential forensic marker for estimating the time passed since death. The results show the BTB-BSA-AuNC system to be capable of detecting respective intracellular pH changes.

**Keywords** pH nanosensor · Bromothymol blue · Red blood cell imaging · Fluorescent nano-materials · Forensic test · Dead blood cells · Bovine serum albumin

## Introduction

Sensing and monitoring pH changes inside living cells can act as a near mark to understand many physiological and pathological processes. The regulation of intracellular pH ( $\text{pH}_i$ ) provides the appropriate environment for many cell functions such as cellular metabolisms [1], cell growth [2], ion transport, enzymes activity, conductivity of ion channels, calcium regulation and others [3]. All normal cells contain intracellular pH ( $\text{pH}_i$ ) and extracellular pH ( $\text{pH}_e$ ) within range of 7.0–7.2 and 7.3–7.4 respectively [4]. It is reported that cancer cells associated with higher  $\text{pH}_i$  7.1–7.7 and lower  $\text{pH}_e$  6.2–6.9 [5]. Thus, monitoring of an abnormal  $\text{pH}_i$  and /or  $\text{pH}_e$  is considered as important hallmark to the progression of cancers or diseases (e.g. Alzheimer's disease). In addition, it represents an indispensable tool for following up the responses of cancer cells to various therapies. Antemortem blood pH is regulated to be within the normal physiological range. After death, reduction of blood pH is expected due to stoppage of the body buffering system. It is reported that pH changes can be used as a marker to estimate the time passed since death significantly. In this regard, almost all previous studies depend on estimation of blood  $\text{pH}_e$  after death with traditional methods [6].

Despite various methods being reported for measuring pH [7, 8], fluorescence based pH sensor has a high rank among other tools for  $\text{pH}_i$  sensing in-vivo and in-vitro [9, 10]. Based on reversible changes in the fluorescence properties of a weak acid or base molecule induced by pH; pH-sensitive organic fluorophores and fluorescent proteins [11] have gained considerable attention in this area. However, they suffer from

**Electronic supplementary material** The online version of this article (doi:10.1007/s00604-017-2352-7) contains supplementary material, which is available to authorized users.

✉ Reham Ali  
Reham.Ali@suezuniv.edu.eg

<sup>1</sup> Chemistry Department, Faculty of Science, Suez University, Suez 43518, Egypt

<sup>2</sup> Chemistry Branch, Department of Science and Mathematics, Faculty of Petroleum and Mining Engineering, Suez University, Suez 43721, Egypt

<sup>3</sup> Department of Forensic Medicine & Clinical Toxicology, Faculty of Medicine, Suez Canal University, Ismailia 41522, Egypt

some drawbacks that can hinder the intracellular pH sensitivity, especially in living tissues. These shortcomings include problems with the intracellular delivery, self-redistribution leakage from cells, interactions with other molecules, cytotoxicity, small Stokes shift and weak photostability [12]. The inevitable limitations of the organic fluorophores led to increase the research for other alternative fluorescent material. A wide variety of nanoparticles have been employed to improve pH assessment, owing to their small size, high surface-to volume ratio, good biocompatibility, greater chemical stability, high signal-to-noise ratio and stability against photo bleaching [13, 14].

Fluorescent noble metal nanoclusters, in particular fluorescent AuNCs, have gathered considerable attention among others luminescent nanoparticles (semiconductor quantum dots (QDs), lanthanide nanoparticles, carbon nanodots, and silica nanoparticles). They provide unique properties such as small size (less than 2 nm), water solubility, photostability, non-toxic, bio-compatibility, and large Stokes shift (about 170 nm) [15, 16]. AuNCs possess electronic structure and distinctive properties different from larger size gold nanoparticles (above 2 nm). AuNCs don't show a size-dependent plasmon absorption like large gold nanoparticles. However, AuNCs possess size dependent fluorescence due to their small size which comparable to Fermi wavelength of the conduction electron that lead to molecule-like properties of discrete electronic states [17]. Various methods have been developed for the syntheses of AuNCs with different emission wavelength; which can be tuned by changing the capping material such as glutathione, proteins and alkanethiol [18, 19]. Many applications based AuNCs have been presented including molecular identification [20] and potential applications in biolabeling [21] imaging and sensing [22].

Water-soluble AuNCs capped with commercial bovine serum albumin (BSA-AuNCs) were prepared using “one-pot” green method [23]. The synthesized nanoclusters provide strong red fluorescent with  $QY \approx 6$  in aqueous solution. Owing to their excellent properties, these AuNCs are promising candidate for biolabeling and bioimaging applications in addition to sensing biological species in the living cells. AuNCs has been reported [24] as a reference signal with a pH-sensitive organic fluorophore for targeted imaging of cancer cells and ratiometric detection of  $pH_i$ . Whereas, AuNCs capped with N-acetyl-L-cysteine showed ultrasensitive pH response within range (6.05–6.4) [25].

This work presents a novel pH nanosensor compatible with pH-intracellular sensing at physiological range. The fluorescent signal of AuNCs overcomes the limitation of using organic fluorophores or other luminescent nanoparticles. However, the emission of BSA-AuNCs is pH independent within range 2–11 so they can't be used as direct pH probes. BSA-AuNCs have luminescence intensity at 640 nm after excitation with 470 nm. The simplest way to modulate the

intensity of the emission of BSA-AuNCs is label them with classical pH indicator. The basic requirement is existence of an overlap between the emission of the AuNCs and the absorbance of the pH indicator, which does not need to be fluorescent. A color change in either strong or weak quenching (absorption) of the AuNCs emission depends on the actual absorbance of the indicator. It is well known that bromothymol blue (BTB) has been widely used as pH indicator in the physiological pH range (6–8) [14, 26]. Its absorption spectra changes according to protonation or deprotonation. BTB has a high binding affinity to protein like BSA [27] and widely used in the protein detection [28]. By binding BTB with BSA; which capped AuNCs, the red emission at 640 nm of AuNCs expected to modulate based on the inner filter effect of BTB, whether it exists in acidic or basic form.

Most of researches related to NCs are directed towards medical applications [21, 29] although they may also be directed towards forensic applications [30]. Therefore, this study also aimed to test the newly constructed pH nanosensor (BTB-BSA-AuNCs) by detecting post-mortem changes in blood  $pH_i$ ; which was obtained from rat corpse over a period of 72 h.

## Experimental

### Reagents and materials

All chemicals were purchased from Sigma Aldrich Co. (<http://www.sigmaldrich.com/european-export.html>), and at the highest purity available. The other reagents and organic solvents were of the highest grade available.

### Apparatus

pH was determined with a digital pH meter (Hanna Instruments, <http://hannainst.com>). The instrument was calibrated at  $20 \pm 2$  °C with standard buffers of pH 7.0 and 4.0. The electronic absorption spectra were recorded in 1 cm quartz cell using Evolution™ 200 series UV-Visible spectrophotometer (<https://www.thermofisher.com>). The excitation and emission spectra were measured with JASCO-FP6300 spectrofluorometer ([www.jascoinc.com](http://www.jascoinc.com)) utilizing 1 cm quartz for all spectral measurements. Transmission electron microscope (TEM) images of BSA-AuNCs were acquired using JEOL-100S Japan (<https://www.jeol.co>) working at 200 kV. Fourier Transform Infrared Spectroscopy (FTIR) spectra were recorded on a 4100 Jasco-Japan ([www.jascoinc.co](http://www.jascoinc.co)) over the wavenumber region 4000 to  $400\text{ cm}^{-1}$ . Fluorescence images of blood samples were collected utilizing fluorescence microscope (FM) Olympus CKX41 inverted microscope, (<https://www.olympus-europa.com>) Tokyo, Japan.

## Preparation of buffers

Doubly distilled water was used for the preparation of 20 mM Britton-Robinson (B. R.) buffer. Different buffers with pH ranging from 4 to 9 was adjusted by pH meter using the same stock solution of the B. R. buffer by adding appropriate amount of 1 M HCl or NaOH solution.

## Preparation of BSA-AuNCs

The BSA- AuNCs were synthesized using a reported method [23]. All glassware was washed with aquaregia, and rinsed with ethanol and ultrapure water. In a typical experiment, aqueous HAuCl<sub>4</sub> solution (5 mL, 10 mM, and 37 °C) was added to BSA solution (5 mL, 50 mg.mL<sup>-1</sup>) under vigorous stirring. After 2 min NaOH solution (0.5 mL, 1 M) added to adjust the pH of the mixture solution to 11.5. The mixture incubated for 12 h under vigorous stirring at 37 °C, wherein the solution turned from pale yellow to brown. The solution after synthesis was dialyzed in ultra-high purity water (changing the water every 8 h) for more than 24 h to remove all small-molecular impurity. After dialysis, the resulting solution of BSA-AuNCs was concentrated to 10 mL and stored in the dark at 4 °C for later use. The concentration for BSA-AuNCs prepared by similar procedure was estimated before as 0.02 M [31]. For characterizations, BSA-AuNCs were freeze-dried and stored at 4 °C.

## Preparation of BTB-BSA-AuNCs

Bromothymol blue sodium salt stock solution was prepared by dissolving 10 mg in 2 mL of water. 0.5 mL of this stock solution was mixed with 3 mL of AuNCs in buffer pH 7.4. The mixture incubated for 1 h at room temperature and then dialysis against ultra-high purity water for 8 h to remove excess dye. For characterizations, freeze dryer was used and the solid BTB-BSA-AuNCs was obtained. Successful binding of BTB-BSA-AuNCs was confirmed by FTIR and UV-Vis absorption spectroscopy.

## Optical studies of pH effects on BTB-BSA-AuNCs

The UV – Vis spectra of BTB-BSA-AuNCs were measured in an aqueous solution of Britton- Robinson (B. R.) buffers at pH 4, 6, and 9. During titration, 50 µL of the prepared BTB-BSA-AuNCs were added to 2 mL of B.R. buffers. The fluorescence spectra were recorded within pH range 4–9 where 100 µL of BTB-BSA-AuNCs were added to 2 mL of Britton-Robinson (B. R.). For all measurements, excitation and emission slit widths were 5 nm.

## The application

### Blood sampling and collection

Blood was obtained from Wistar albino rats stored in corpses. Bloods were collected in heparinized tubes as it is previously recommended in order to not affect the delivery of BTB-BSA-AuNCs by blood cells [32].

### Measurements of pH after death at different time interval

pH<sub>e</sub> was measured in blood at different time interval (directly after death, at 24, 48 and 72 h after death) by using digital pH meter. At each interval and for measuring pH<sub>i</sub>, 25 µL of collected blood were left to dry on clean glass slide. 25 µL of BTB-BSA-AuNCs were added to the dried blood on the slide then both were incubated for around 5 h [21].

## Results and discussion

### Choice of materials

We present a pH nanosensor based on fluorescent BSA-AuNCs. The nanoclusters were synthesized by previously reported method through the reduction of HAuCl<sub>4</sub> using BSA as capping and reducing agent. The tyrosine residue of BSA is responsible for reducing Au<sup>3+</sup> to Au<sup>0</sup> at pH 11.0 [33]. In sequence, cystien residues in BSA stabilize the Au-S bonding. Figure 1 shows TEM images of the BSA-AuNCs which give typical result with an average size of 2 nm.

The prepared BSA-AuNCs shows several advantages over other organic dyes and luminescent nanomaterials such as eco-friendly synthesis, water solubility, ultrasmall size, high quantum yield, good photostability and biocompatibility. Additionally, they exhibit large Stokes shift (170 nm) which reduced the reabsorption of emitted light and prevent scattering. All these advantages make BSA-AuNCs a perfectly suited candidate for detecting pH in medical applications. The

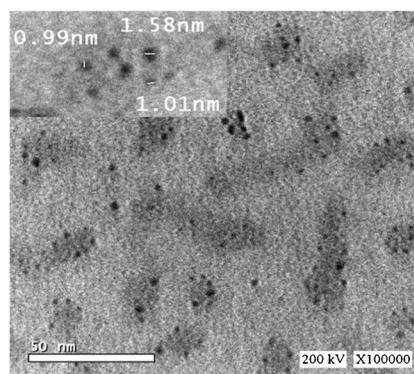
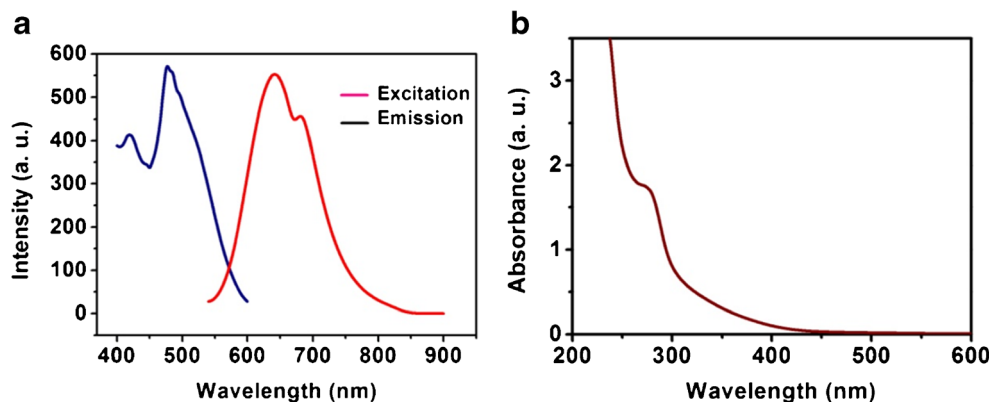


**Fig. 1** Transmission electron microscopy pictures of the BSA-AuNCs

**Fig. 2** **a** Fluorescence excitation (emission at 640) and emission (excitation at 470). **b** Absorption spectra of aqueous solution of BSA- AuNCs



absorption spectrum of BSA-AuNCs in aqueous solution is shown in Fig. 2b; the absence of a surface plasmon peak around 520 nm indicates that no nanoparticles were formed. The BSA-AuNCs show strong emission centered at 640 nm upon excitation at 470 nm. The excitation and emission spectra are shown in Fig. 2a. The BSA-AuNCs itself is insensitive to the pH in the range 3–9 as shown in Fig. S1.

A longwave pH indicator BTB is chosen due to nontoxicity and covering the physiological range. At basic pH values, BTB undergoes a large absorption spectral shift from yellow at pH 4 via green (pH 6–7) to blue (at pH 9.0) (as shown in Fig. 3) and it is nonfluorescent. The absorption spectrum of the dye (in the range 500–700) has a strong overlap with the red emission of BSA-AuNCs (with maxima at 640 nm) as shown in Fig. 3. With increasing pH, the absorption of the dye in the range 500–700 nm increases which was expected to show a significant inner filter effect on the emission of BSA-AuNCs upon excitation with 470 nm.

On the other hand, the absorption of BTB does not considerable change in the range 500–700 nm at different pH (5, 7, and 9) compared to the absorption of BTB in the presence of BSA-AuNCs. Figure 4 indicates that there is no change in the pH of the solution upon addition of BSA-AuNCs.

It has been demonstrated that BTB molecules can be adsorbed noncovalently or statically on the surfaces of

BSA-AuNCs. This has been proved from severe quenching of BSA fluorescence in the presence of BTB [27]. A combination of the electrostatic and  $\pi$ - $\pi$  interactions between the negative BTB moieties and the positive groups of BSA molecules controlled the interaction between BTB and BSA-AuNCs. The binding between BTB and BSA as reported before is nearly 100% bound. Analysis of binding revealed that five molecules of bromothymol blue bound very strongly to a molecule of rabbit albumin at pH 7.4 [28]. The interaction of BTB with HSA was carried out to form an electrochemical non-active complex BTB-HSA by electrostatic and other weak forces [34]. The binding of BTB to surface of AuNCs can be attributed to the presence of un-reduced surface Au<sup>+</sup> ions (about 17%). This undergoes a strong and specific interaction with BTB [22, 23].

#### Structural characterization of BTB labeled AuNCs.

FT-IR is a spectroscopic technique that can be characterized sensitivity of nanomaterial surface by proceeding in reflectance mode. Thus, FT-IR was utilized to examine the nanofluorosensor particles to determine the extent of structural changes. FT-IR spectra were recorded for BTB and BSA-AuNCs before and after incubation with BTB as shown in

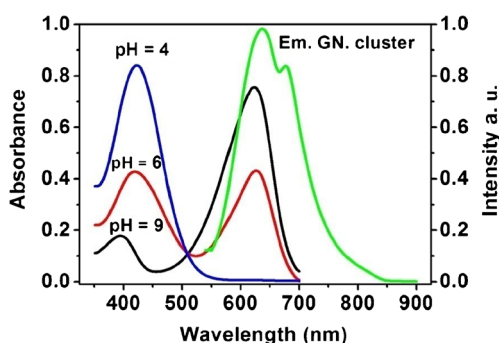


**Fig. 3** Absorption spectra of bromothymol blue at different pH in aqueous solution and the emission band of the BSA-AuNCs upon excitation at 470 nm

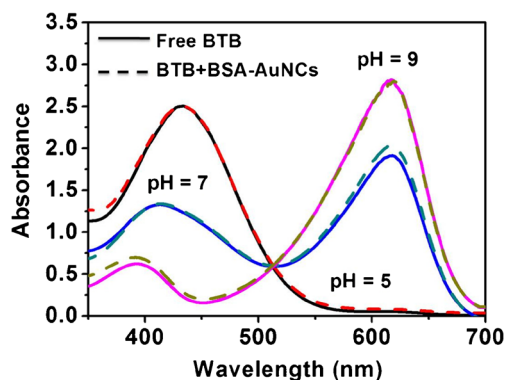


**Fig. 4** Absorption spectra of bromothymol blue at different pH range of (5, 7 and 9) in aqueous solutions and in presence of BSA-AuNCs



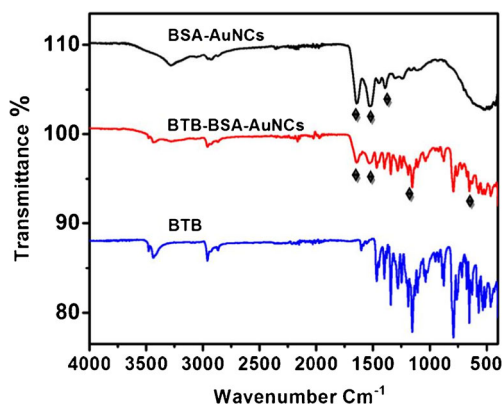


**Fig. 5** FT-IR spectra of BTB, BSA-AuNCs and BSA-AuNCs labeled BTB

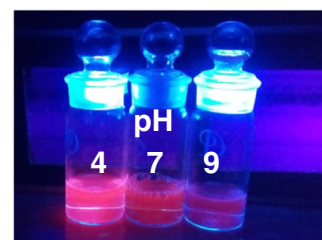
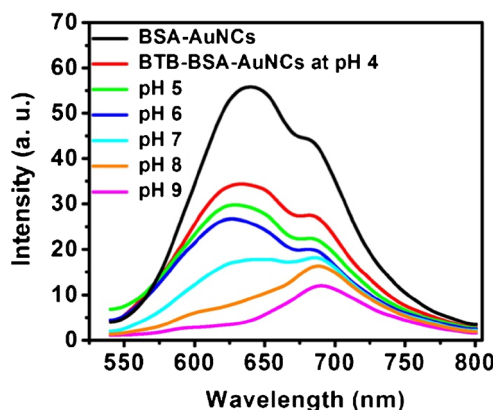
**Fig. 5.** In the spectrum of BSA-AuNCs plain particles, the most intense peaks are located at  $1648\text{ cm}^{-1}$ ,  $1536\text{ cm}^{-1}$ , and  $1388\text{ cm}^{-1}$ , these peaks are due to the amide-I band C = O stretching vibration, N–H bending vibration and the C–N stretching mode respectively. These results give a strong evidence for the presence of BSA linked to surface of gold nano-cluster. Therefore, we can attribute the existence of new bands to BTB adsorbed on the BSA-AuNCs surface. In comparison to FT-IR of BTB coupled BSA-AuNCs particles, the spectrum exhibits bands at  $1197\text{ cm}^{-1}$  and  $1023\text{ cm}^{-1}$  which are assigned to  $-\text{SO}_3$  [35]. The band locating at  $659\text{ cm}^{-1}$  is due to Br–C stretching vibrations. The presence of the main characterized peaks of the pure BTB is a strong evidence for surface adsorption process. So far, the FT-IR results designate BTB adsorption onto surface of BSA-AuNCs successfully.

### Studies of pH effect on BTB-BSA-AuNCs

Britton-Robinson (B. R.) 5 mM was used to study the pH effect within the range of (4–9). The fluorescence spectra of BTB-BSA-AuNCs were recorded at different pH. Further, a decrease in the emission intensity at 640 nm was observed with increasing the pH (Fig. 6).

The fluorescence intensity of BSA-AuNCs at 640 nm under an excitation wavelength of 470 nm was quenched

**Fig. 6** The effect of pH on the emission intensity of BTB-BSA-AuNCs under an excitation wavelength of 470 nm and within pH range (4–9) and Photographs under UV light of BTB-BSA-AuNCs at pH 4, 7 and 9



significantly about 36% compared to emission of BTB-BSA-AuNCs at pH 4 although the absorption of BTB in this range significantly is very weak. However, this behavior can be attributed to the interaction between BTB and BSA-AuNCs. The absorption band of BTB didn't show any significant change in the presence of BSA-AuNCs, suggesting that there is no change in the pH of the solution upon addition of BSA-AuNCs as shown in Fig. 4.

### Stability and response of BTB-BSA-AuNCs

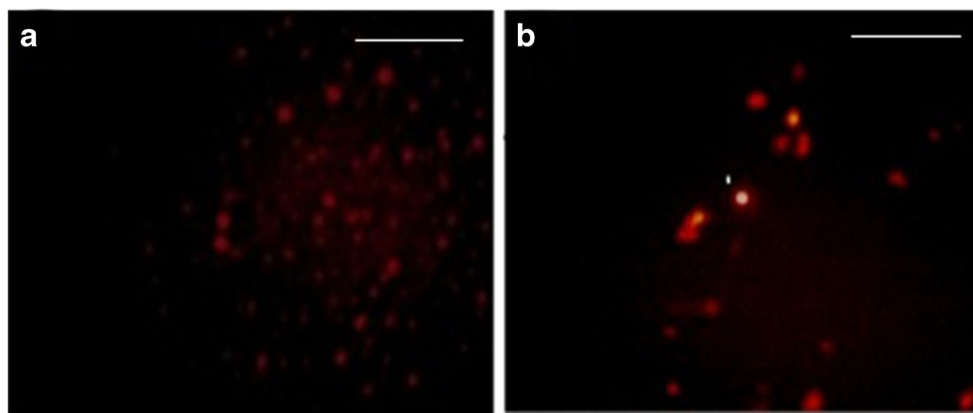
No obvious change in fluorescence properties was observed for BTB-BSA-AuNCs in solutions with a high salt concentration (e.g., 1 M NaCl) see Fig. S2a. Also, same study was carried out in presence of different concentrations of protein to detect any changes in the fluorescence property of the BTB-BSA-AuNCs. The histidine was utilized in range of 0 to 250 mM. It is found that there are no actual changes in fluorescence of BTB-BSA-AuNCs upon addition of histidine with different concentrations (Fig. S2b).

The response of BTB-BSA-AuNCs pH sensor was investigated in aqueous solutions. The pH value of the medium was controlled using acid or base addition. Fig. S3 exhibits the response curve of the BTB-BSA-AuNCs. Repetitive cycling between an approximately pH of 6 to 8 were performed. For that purpose, the Good reversibility, with almost no change in fluorescence intensity of BTB-BSA-AuNCs is observed. The fast response of the pH-nanosensor AuNCs towards changes in pH is in the order of several seconds, obviously because of its small size and high hydrophilicity.

### Estimation of $\text{pH}_i$ based on BTB-BSA-AuNCs

Initial postmortem changes can only be detected biochemically as the metabolism in the cells alters to autolytic pathways. Thus, it is reported that pH changes can be used as a marker to estimate early time based since death [6]. The early time since death based on  $\text{pH}_e$  changes was detected previously at 24 and 96 h after death. In the present study, very minimal

**Fig. 7** Fluorescent microscopic images of rat blood cells labeled with BTB-BSA-AuNCs. Blood was obtained from rat corpse (a) directly after death (b) 72 h after death. Scale bar = 100  $\mu\text{m}$



changes in rat blood  $\text{PH}_e$  were detected at 0, 24, 48 h after death ( $\text{PH}_e$  were 6.76, 6.63, 6.61 respectively). Then,  $\text{PH}_e$  reduced to 5.04 at 72 h after death as shown in Fig. S4. There is no detected difference in intensity of red fluorescence corresponds to the BTB-BSA-AuNCs at 0, 24 and 48 h after death. While red fluorescence increased with pH reduction at 72 h after death (Fig. 7). This occurs due to accumulation of acidic cellular metabolites such as hydrogen ions, carbon dioxide, formic acid and lactic acid generated inside cells [6]. Autolysis of blood cells is most probably the reason behind reducing the observed number of labeled blood cells with increasing time passed since death. Moreover, the different types of blood cells degrade at different time interval after death. [36]

Table S1 lists the recently reported nanomaterial based intracellular pH sensing. All pH sensors presented in the table have certain features. The present pH Nano-sensor inherits attractive features as compared to other reported pH sensors due to ultra-small size with good biocompatibility due to both the Au core (which is inert) and BSA shell which has good biocompatibility. Additionally, the pH values of solutions or cells are detected based on the red luminescence of the present nanoclusters which occurred in the near infra-red region with a large Stokes shift (170 nm) to reduced the reabsorption of emitted light and prevent scattering. The present nanosensor has a good stability, sensitivity and reversibility.

## Conclusions

In conclusion, we developed a new pH nano-fluorosensor based on gold nanocluster with a diameter of 2 nm. The pH sensor has attractive features including ultra-small size, high quantum yield with large Stokes shift, good photostability and biocompatibility. The BTB is easily linked to the surface of BSA capped gold nanoparticles non-covalently. The sensor response was detected in pH range of 4–9. The effect of salinity and protein on the sensor stability was studied and the pH sensor shows a high stability in aqueous medium. The present

study shows that BTB-BSA-AuNCs able to detect changes in blood pH<sub>i</sub> and can be a helpful forensic tool for estimating early time passed since death. Further, various other labels of sensing materials (in terms of pH probes, polymers, and additives) that may be used in the future to adjust such sensors to the specific needs of sensing and bio-sensing.

**Compliance with ethical standards** The author(s) declare that they have no competing interests.

## References

1. Busa WB, Nuccitelli R (1984) Metabolic regulation via intracellular pH. *Am J Physiol Regul Integr Comp Physiol* 246:R409–R438
2. Putney LK, Barber DL (2003) Na-H exchange-dependent increase in intracellular pH times G2/M entry and transition. *J Biol Chem* 278:44645–44469
3. Madshus IH (1988) Regulation of intracellular pH in eukaryotic cells. *Biochem J* 250:1–8
4. Walenta S, Wetterling M, Lehrke M, Schwickert G, Sundf r K, Rofstad EK, Mueller-Klieser W (2000) High lactate levels predict likelihood of metastases, tumor recurrence, and restricted patient survival in human cervical cancers. *Cancer res* 60:916–921
5. Damaghi M, Wojtkowiak JW, Gillies RJ (2013) pH sensing and regulation in cancer. *Front Physiol* 4:370
6. Donaldson AE, Lamont IL (2013) Biochemistry changes that occur after death: potential markers for determining post-mortem interval. *PLoS One* 8:e82011
7. Hesse SJ, Ruijter GJ, Dijkema C, Visser J (2000) Measurement of intracellular (compartmental) pH by <sup>31</sup>P NMR in *Aspergillus niger*. *J Biotechnol* 77:5–15
8. Orgovan G, Noszal B (2011) Electrodeless, accurate pH determination in highly basic media using a new set of (<sup>1</sup>H NMR pH indicators. *J Pharm Biomed Anal* 54:958–964
9. Li Y, Wang Y, Yang S, Zhao Y, Yuan L, Zheng J, Yang R (2015) Hemicyanine-based high resolution ratiometric near-infrared fluorescent probe for monitoring pH changes in vivo. *Anal Chem* 87: 2495–2503
10. Zhou X, Su F, Lu H, Senechal-Willis P, Tian Y, Johnson RH, Meldrum DR (2012) An FRET-based ratiometric chemosensor for in vitro cellular fluorescence analyses of pH. *Biomaterials* 33:171–180

11. Bizzarri R, Serresi M, Luin S, Beltram F (2009) Green fluorescent protein based pH indicators for in vivo use: a review. *Anal Bioanal Chem* 393:1107–1122
12. Keith BM, Bernard L, Sabahudin H, Geoff S, John HT (2008) Assessment of cytotoxicity of quantum dots and Gold nanoparticles using cell-based Impedance Spectroscopy. *Anal Chem* 80:5487–5493
13. Knopp D, Tang D, Niessner R (2009) Review: bioanalytical applications of biomolecule-functionalized nanometer-sized doped silica particles. *Anal Chim Acta* 647:14–30
14. Sun LN, Peng H, Stich MI, Achatz D, Wolfbeis OS (2009) pH sensor based on upconverting luminescent lanthanide nanorods. *Chem Commun (Camb)* 33:5000–5002
15. Chen LY, Wang CW, Yuan Z, Chang HT (2015) Fluorescent gold nanoclusters: recent advances in sensing and imaging. *Anal Chem* 87:216–229
16. Khandelia R, Bhandari S, Pan UN, Ghosh SS, Chattopadhyay A (2015) Gold Nanocluster embedded albumin nanoparticles for two-photon imaging of cancer cells accompanying drug delivery. *Small* 11:4075–4081
17. Lee D, Donkers RL, Wang G, Harper AS, Murray RW (2004) Electrochemistry and optical absorbance and luminescence of molecule-like Au<sub>38</sub> nanoparticles. *J Am Chem Soc* 126:6193–6199
18. Negishi Y, Nobusada K, Tsukuda T (2005) Glutathione-protected gold clusters revisited: bridging the gap between gold(I)-thiolate complexes and thiolate-protected gold nanocrystals. *J Am Chem Soc* 127:5261–5270
19. Xu Y, Sherwood J, Qin Y, Crowley D, Bonizzoni M, Bao Y (2014) The role of protein characteristics in the formation and fluorescence of Au nanoclusters. *Nano* 6:1515–1524
20. Wang M, Mei Q, Zhang K, Zhang Z (2012) Protein-gold nanoclusters for identification of amino acids by metal ions modulated ratiometric fluorescence. *Analyst* 137:1618–1623
21. Lin CAJ, Yang TY, Lee CH, Huang SH, Sperling RA, Zanella M, Li JK, Shen JL, Wang HH, Yeh HI, Parak, WJ, Chang WH (2009) Synthesis, characterization, and bioconjugation of fluorescent gold nanoclusters toward biological labeling applications. *ACS Nano* 3:395–401
22. Xie J, Zheng Y, Ying JY (2010) Highly selective and ultrasensitive detection of Hg<sup>(2+)</sup> based on fluorescence quenching of Au nanoclusters by Hg<sup>(2+)</sup>-Au<sup>(+)</sup> interactions. *Chem Commun (Camb)* 46:961–963
23. Xie J, Zheng Y, Ying JY (2009) Protein-directed synthesis of highly fluorescent gold nanoclusters. *J Am Chem Soc* 131:888–889
24. Ding C, Tian Y (2014) Gold nanocluster-based fluorescence biosensor for targeted imaging in cancer cells and ratiometric determination of intracellular pH. *Biosens Bioelectron* 65C:183–190
25. Deng HH, Wu GW, Zou ZQ, Peng HP, Liu AL, Lin XH, Xia XH, Chen W (2015) pH-sensitive gold nanoclusters: preparation and analytical applications for urea, urease, and urease inhibitor detection. *Chem Commun (Camb)* 51:7847–7850
26. Ali R, Saleh SM, Meier RJ, Azab HA, Abdelgawad I, Wolfbeis OS (2010) Upconverting nanoparticle based optical sensor for carbon dioxide. *Sens Actuators B Chem* 150:126–131
27. Vidal E, Palomeque ME, Lista AG, Fernandez Band BS (2003) Flow injection analysis: Rayleigh light scattering technique for total protein determination. *Anal Bioanal Chem* 376:38–41
28. Zhou XC, Yan CQ, Yan CN (2010) Study on the interaction of bromothymol blue and bovine serum albumin[J]. *Chemical Research and Application* 1:003
29. Lin CA, Lee CH, Hsieh JT, Wang HH, Li JK, Shen JL, Chan WH, Yeh HI, Chang WH (2009) Review: synthesis of fluorescent metallic nanoclusters toward biomedical application: recent progress and present challenges. *J Med Biol Eng* 29:276–283
30. Chakraborty D, Rajan G, Isaac R (2015) A splendid blend of nanotechnology and forensic Science. *Journal of Nanotechnology in Engineering and Medicine* 6:010801–010806
31. Chang HC, Ho JA (2015) Gold Nanocluster-assisted fluorescent detection for hydrogen peroxide and cholesterol based on the inner filter effect of gold nanoparticles. *Anal Chem* 87:10362–10367
32. Baumann D, Hofmann D, Nullmeier S, Panther P, Dietze C, Musyanovych A, Ritz S, Landfester K, Mailänder V (2013) Complex encounters: nanoparticles in whole blood and their uptake into different types of white blood cells. *Nanomedicine* 8:699–713
33. Hsu NY, Lin YW (2016) Microwave-assisted synthesis of bovine serum albumin-gold nanoclusters and their fluorescence-quenched sensing of Hg<sup>2+</sup> ions. *New J Chem* 40:1155–1161
34. Wang XL, Jie YA, Kui JI (2008) Electrochemical study on the interaction of protein with Bromothymol blue and its analytical application. *Chem Res Chin Univ* 24:701–706
35. Silverstein RM, Webster FX, Kiemle DJ (2005) Spectrometric identification of organic compounds. Wiley, New Delhi, pp 107–108
36. Donaldson AE, Lamont IL (2014) Estimation of post-mortem interval using biochemical markers. *Aust J Forensic Sci* 46:8–26